Т. 85, № 4 **ЖУРНАЛ ПРИКЛАДНОЙ СПЕКТРОСКОПИИ** ИЮЛЬ — АВГУСТ 2018

V. 85, N 4 **JOURNAL OF APPLIED SPECTROSCOPY** JULY — AUGUST 2018

RED AND YELLOW LUMINESCENCE OF Eu^{3+}/Dy^{3+} CO-DOPED HYDROXYAPATITE/β-TRICALCIUM PHOSPHATE SINGLE PHOSPHORS SYNTHESIZED USING COPRECIPITATION METHOD[**]

Hoang Nhu Van, Phuong Dinh Tam, Vuong-Hung Pham[*]

Advanced Institute for Science and Technology, Hanoi University of Science and Technology,
No. 01, Dai Co Viet, road, Hanoi, Vietnam; e-mail: vuong.phamhung@hust.edu.vn

This paper reports the first attempt at the synthesis of single phosphors of europium (Eu^{3+}) and dysprosium (Dy^{3+}) co-doped hydroxyapatite (HA)/β-tricalcium phosphate (TCP) nanostructures providing strong red and yellow luminescence depending on annealing temperature and holding time. The morphology of the phosphors was observed to have a nanowire structure. The photoluminescence (PL) intensity of the phosphors increases with annealing temperature and time. The luminescent phosphors also showed the typical luminescence of Eu^{3+} centered at 610 nm and Dy^{3+} centered at 572 nm, which was more efficient for the annealed Eu^{3+}/Dy^{3+} co-doped HA/TCP phosphors than for as-synthesized ones. These results suggest that the Eu^{3+} and Dy^{3+} co-doped HA/TCP nanostructures can find potential application in plant cultivation as environment friendly phosphors.

Keywords: *dysprosium, luminescence, hydroxyapatite, europium, nanophosphor, nanobiophosphor.*

КРАСНОЕ И ЖЕЛТОЕ СВЕЧЕНИЕ СИНТЕЗИРОВАННЫХ МЕТОДОМ СОВМЕСТНОГО ОСАЖДЕНИЯ ОДНОКОМПОНЕНТНЫХ ЛЮМИНОФОРОВ НА ОСНОВЕ СОЛЕГИРОВАННОГО ИОНАМИ Eu^{3+}/Dy^{3+} ГИДРОКСИАПАТИТА/β-ТРИКАЛЬЦИЯ ФОСФАТА

H. N. Van, Ph. D. Tam, V.-H. Pham[*]

УДК 535.37

Ведущий научно-технический институт, Ханойский университет науки и технологии,
Ханой, Вьетнам; e-mail: vuong.phamhung@hust.edu.vn

(Поступила 28 ноября 2016)

Представлены результаты синтеза наноструктур однокомпонентных люминофоров на основе солегированного ионами Eu^{3+} и Dy^{3+} гидроксиапатита (ГА)/β-трикальция фосфата (ТКФ), обеспечивающих интенсивное красное и желтое свечение, зависящее от температуры и длительности отжига. Морфологические исследования показали, что люминофоры обладают нанопроволочной структурой. Интенсивность их фотолюминесценции возрастает с температурой и длительностью отжига. Для полученных люминофоров наблюдалась типичная для Eu^{3+} и Dy^{3+} люминесценция с максимумами при 610 и 572 нм, которая оказалась более эффективной у подверженных отжигу образцов ГА/ТКФ, солегированных ионами Eu^{3+}/Dy^{3+}, чем у только что синтезированных образцов. Показана перспективность применения солегированных ионами Eu^{3+} и Dy^{3+} ГА/ТКФ наноструктур в качестве экологически безвредных люминофоров.

Ключевые слова: *диспрозий, люминесценция, гидроксиапатит, европий, нанолюминофор, нанобиолюминофор.*

[**] Full text is published in JAS V. 85, No. 4 (http://springer.com/10812) and in electronic version of ZhPS V. 85, No. 4 (http://www.elibrary.ru/title_about.asp?id=7318; sales@elibrary.ru).

Introduction. The development of new phosphors for artificial illumination conditions in agriculture lighting plays a significant role in designing the plant factory (the so-called green crop production system) due to its outstanding properties of high yields, safety, environmental friendliness, and non-pollution without pesticides and chemical fertilizers [1–3]. A synthetic light source with red and blue emission is beneficial to growth and development of plants [4, 5]. It is well known that the flowering and seed yield of some fruits can be increased under the specific lighting technique [6, 7]. For example, blue [8, 9], red [10–12], and yellow light [13, 14] has been used to illuminate plants, which can significantly enhance plant cultivation. Therefore, considerable efforts have been made to functionalize phosphors that can emit light in spectral regions favorable to the plant growth and development [14, 15].

The combination of the advantages of environmental friendly properties with specific luminescence of phosphors is particular of interest to the development of optoelectronic devices for agriculture lighting. As a biocompatible material, hydroxyapatite (HA) has received considerable attention as a host material in designing luminescence materials because HA can incorporate a wide variety of substitutions for Ca^{2+} and PO_4^{3-} and/or OH^- ion based on the flexibility of the apatite structure [16, 17]. Nevertheless, there are only a few reports on the effect of dysprosium doped hydroxyapatite [18, 19]. In particular, to our knowledge, there are no reports on the red and yellow dual luminescence of Eu^{3+}/Dy^{3+} doped HA/TCP for plant cultivation. Recently, strong red light emission has been obtained from Eu doped hydroxyapatite and silicon-substituted hydroxyapatite synthesized successfully in our laboratory by the coprecipitation method [20–22]. To expand this research, we herein report for the first time both red and yellow light emission from Eu^{3+}/Dy^{3+} co-doped HA/TCP synthesized using the co-precipitation method. The crystal structure of the specimen was characterized by X-ray diffraction. The microstructure and chemical composition of the Eu^{3+}/Dy^{3+} doped HA/TCP were characterized the transmission electron microscope (TEM) and field emission scanning electron microscopy (FE-SEM). The optical properties of the phosphor were also determined by a photoluminescence spectrometer.

Experimental procedure. Europium and dysprosium co-doped HA/TCP was synthesized through a co-precipitation method, as follows. An aqueous solution with a stoichiometric amount of $(NH_4)_2HPO_4$ (0.2 M, 99.9% purity, Aldrich) was added to an aqueous solution containing $Ca(NO_3)_2 \cdot 4H_2O$ (0.2 M, 99.9% purity, Aldrich), $Dy(NO_3)_3$, and $Eu(NO_3)_3$ solutions. $Dy(NO_3)_3$ and $Eu(NO_3)_3$ were obtained by dissolving Dy_2O_3 (99.9% purity, Aldrich) and 0.4 g Eu_2O_3 (99.9% purity, Aldrich) in dilute HNO_3 with vigorous stirring. The concentration of $Eu(NO_3)_3$ was kept constant, while the concentration of $Dy(NO_3)_3$ was varied to control the luminescent properties. The reaction mixture was stirred for 0.5 h followed by the precipitation method at 80°C, and the pH was adjusted to 11 using aqueous ammonia. The resulting precipitates were washed three times and then dried at 100°C for 6 h (as-received sample). A fraction of each as-prepared sample was treated at 600, 800, 900, 1000, and 1100°C for 1 h in air. The crystal structures of the Eu^{3+}/Dy^{3+} co-doped HA/TCP were characterized by X-ray diffraction (XRD, D8 Advance, Bruker, Germany). The microstructure and chemical composition of the Eu^{3+}/Dy^{3+} co-doped HA/TCP were determined by transition electron microscope (JEOL, JEM 1010, JEOL Techniques, Tokyo, Japan) and field emission scanning electron microscopy (JEOL, JSM-6700F, JEOL Techniques, Tokyo, Japan). Photoluminescence (PL) tests were performed to evaluate the optical properties of the Eu^{3+}/Dy^{3+} co-doped HA/TCP. A NANO LOG spectrofluorometer (Horiba, USA) equipped with a 450 W Xe arc lamp and double excitation monochromators was used. The PL spectra were recorded automatically during the measurements.

Results and discussion. Figure 1 show an XRD diagram of the as-synthesized Eu^{3+}/Dy^{3+} co-doped HA/TCP and Eu^{3+}/Dy^{3+} co-doped HA/TCP prepared by co-precipitation with thermal annealing of 1100°C and Dy concentration of 1 mol.%. All of the XRD patterns showed a mixture of HA (PDF 01-084-1998) and β-tricalcium phosphate (β-TCP) (PDF 09-0169) with good crystallinity. However, it should be noted that the as-received Eu^{3+}/Dy^{3+} co-doped HA/TCP showed a relatively strong HA (Fig. 1a). On the other hand, when the thermal annealing temperature of 1000°C was applied, a dominant β-TCP peak was observed (Fig. 1b). It can also be seen that the XRD diagram obtained for the Eu^{3+}/Dy^{3+} co-doped HA/TCP samples does not reveal the presence of any phases related to Eu and Dy species, suggesting the successful preparation of the Eu and Dy doped HA/TCP. Based on the specific application, controlling the phase composition of calcium phosphate is of particular interest. The HA and β-TCP phase combination in the specimens may suggest a better performance in the environmental friendly phosphors because of the strong luminescence and good biocompatibility of the β-TCP host [20, 23].

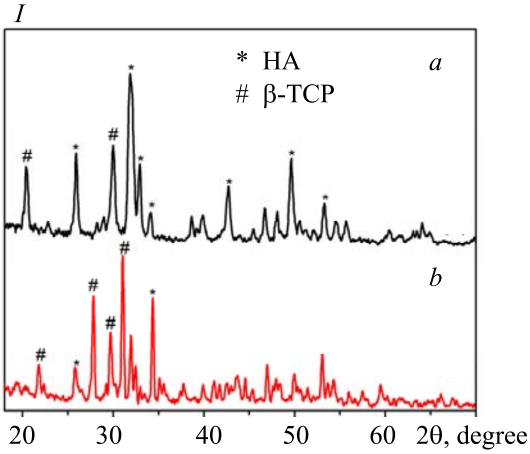

Fig. 1. XRD patterns of the as-synthesized Eu^{3+}/Dy^{3+} co-doped HA/TCP (a) and Eu/Dy codoped HA/TCP (b) at thermal annealing of 1000 °C.

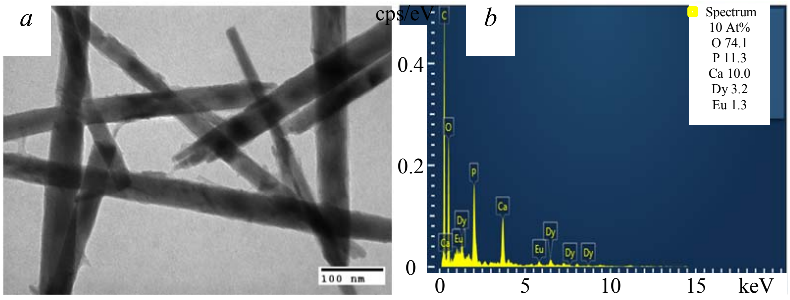

Fig. 2. Microanalysis of the as-received Eu^{3+}/Dy^{3+} co-doped HA/TCP prepared by the co-precipitation method (a), and TEM image and EDS analysis of chemical composition of specimens (b).

The representative microstructure and chemical composition of the as-received Eu^{3+}/Dy^{3+} co-doped HA/TCP were characterized by TEM and EDS, as shown in Fig. 2. The specimen showed a long nanowire microstructure (Fig. 2a) with a length of 700 nm and diameter of 40 nm. Peaks corresponding to the Eu and Dy elements were observed (Fig. 2b), indicating the presence of Eu and Dy in the HA/TCP. In addition, the calculated atomic concentration of the Eu and Dy incorporated was as low as ~1.3 and 3.2%, respectively, which suggests successful doping of Eu and Dy ions into the host HA/TCP. The presence of the C peak in the EDS spectrum was high because the powders were attached on a conductive C tape for the SEM and EDS analysis.

Figure 3 shows the emission spectra of the Eu^{3+}/Dy^{3+} co-doped HA/TCP phosphor with Dy concentration of 1 mol.% annealed at different temperatures monitored at 393 nm. All the Eu^{3+}/Dy^{3+} co-doped HA/TCP showed strong visible emission peaks appearing at about 590, 616, 650, and 700 nm, and they can be attributed to the $^5D_0$–$^7F_1$, $^5D_0$–$^7F_2$, $^5D_0$–$^7F_3$, and $^5D_0$–$^7F_4$ transitions within the Eu^{3+} ion, respectively. The characteristic emission peaks observed at 482 and 572 nm correspond to transitions $^4F_{9/2}$–$^6H_{15/2}$ and $^4F_{9/2}$–$^6H_{13/2}$, indicating the presence of Dy^{3+} ion activating as the luminescence center in the phosphors. However, it should be noted that the relative PL intensity of the phosphors increased by increasing the annealing temperature, and they reached the maximum value at 1100°C. This significant increase in PL was mainly attributed to the presence of the β-TCP phase in the HA/β-TCP system, which can be explained by the absence of hydroxyl (OH^-) groups that constitute possible quenching centers for the luminescence of the Eu^{3+}/Dy^{3+} co-doped HA/TCP phosphors [20, 23].

Figure 4 shows the emission spectra of the Eu^{3+}/Dy^{3+} co-doped HA/TCP phosphor annealed at 1100°C with variation of Dy concentrations monitored at 393 nm. It can be seen that the intensity of the PL increased with increase in Dy concentration when the Dy concentration was 1%. They reached the maximum value and then decreased with further increase in concentration due to concentration quenching effects. More specifically, there was the optimum distance between neighboring Dy^{3+} ions in the host matrix at Dy concentration of 1 mol.% that prevents nonradioactive concentration quenching resulting in the enhancement of PL.

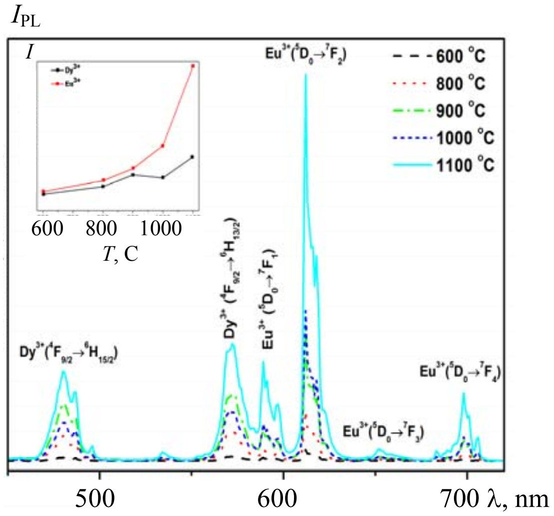

Fig. 3. Photoluminescence spectra of the Dy^{3+}/Eu^{3+} co-doped HA/TCP with Dy concentration of 1 mol.% annealed at different temperatures.

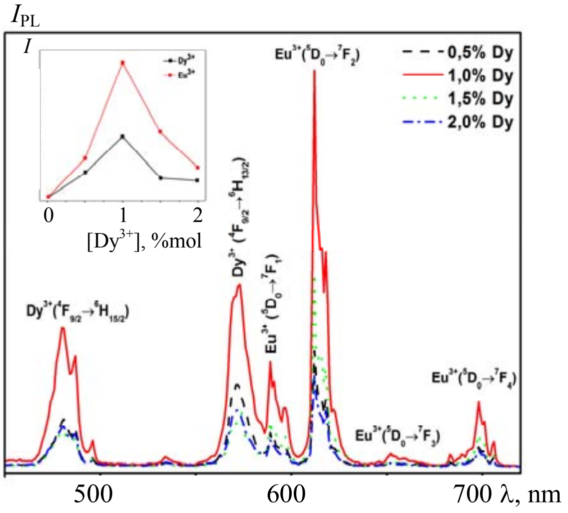

Fig. 4. Photoluminescence spectra of the Eu^{3+}/Dy^{3+} co-doped HA/TCP phosphor as a function of Dy concentrations.

Figure 5 shows the emission spectra of the Eu^{3+}/Dy^{3+} co-doped HA/β-TCP phosphor annealed at 1100°C with different holding times monitored at 393 nm. Similar to the annealing temperature effect, the luminescence of the Eu^{3+}/Dy^{3+} co-doped HA/TCP showed two strong visible emission ranges at red and yellow appearing at about (590, 616, 650, 700 nm) for the red and (482 and 572 nm) for the yellow, which were attributed to the transitions between energy levels within Eu^{3+} ion and Dy^{3+} ion, respectively. However, it can be seen that the PL intensity increased with increase in holding time. When the holding time was 60 min, they reached the maximum value and then decreased further with time. This PL characteristic of the Eu^{3+}/Dy^{3+} co-doped HA/TCP was mainly attributed to concentration quenching of Eu and Dy in the Eu^{3+}/Dy^{3+} co-doped HA/TCP phosphors [21, 24, 25]. More specifically, during the first 5 min to 60 min, there was enough distance between neighboring Eu or Dy ions in the host matrix, which prevents the nonradioactive concentration quenching resulting in enhancing PL.

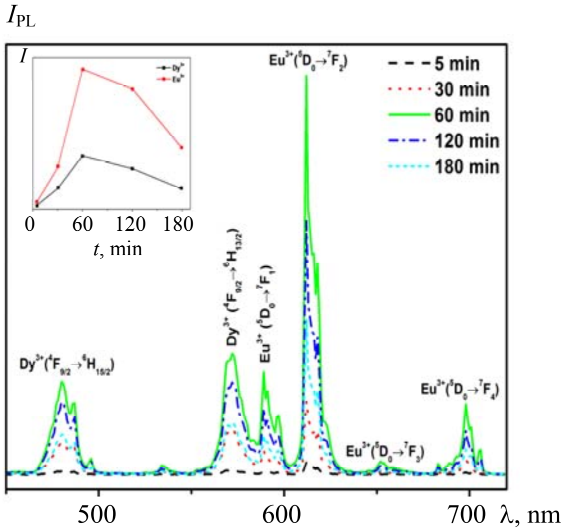

Fig. 5. Photoluminescence spectra of the Eu^{3+}/Dy^{3+} co-doped HA/TCP annealed at 1100°C with different holding times.

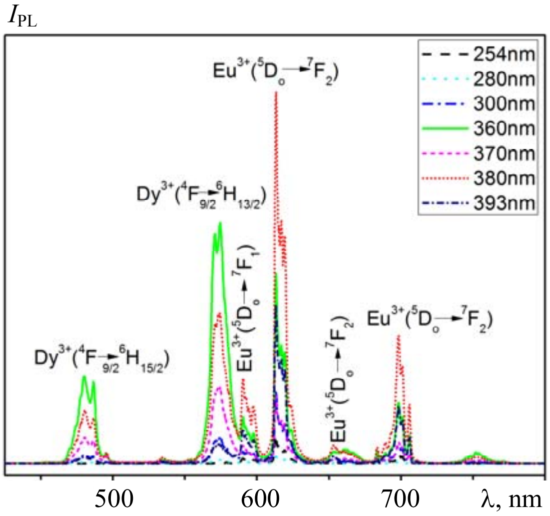

Fig. 6. Photoluminescence spectra of the Eu^{3+}/Dy^{3+} co-doped HA/TCP phosphor with Dy concentration of 1 mol.% annealed at 1100°C as a function of excitation wavelength.

The photoluminescence of the Eu^{3+}/Dy^{3+} co-doped HA/TCP phosphor with Dy concentration of 1 mol.% annealed at 1100°C as a function of excitation energy was further characterized, as shown in Fig. 6. When the phosphors were excited at the excitation wavelengths from 254 to 360 nm, the yellow emission gradually increased, accompanied by decreased red emission intensities. However, when the phosphors were excited at the excitation wavelength of 370–393 nm, the yellow emission decreased, accompanied by increased red emission. This PL characteristics of the phosphors were mainly attributed to activation of different emission centers in the Eu^{3+}/Dy^{3+} co-doped HA/TCP.

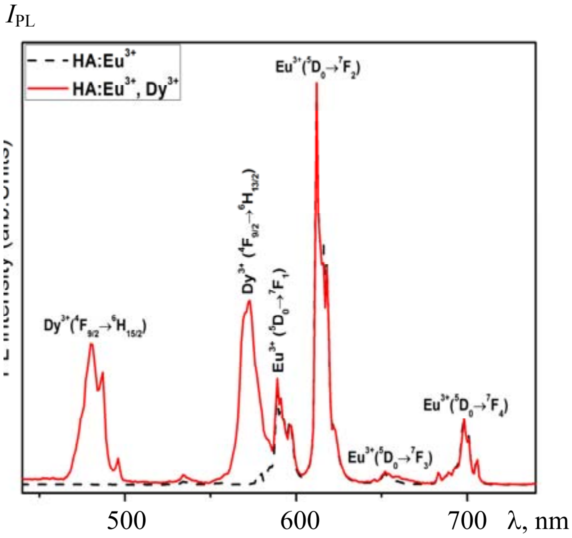

Fig. 7. Photoluminescence spectra of the Eu^{3+} doped HA/TCP and Eu^{3+}/Dy^{3+} co-doped HA/TCP annealed at 1100°C.

The luminescence of the phosphors synthesized without and with the addition of Dy in the coprecipitation process is shown in Fig. 7. The phosphor synthesized without the addition of Dy showed peaks at about 590, 616, 650, and 700 nm, which can be attributed to the $^5D_0$–$^7F_1$, $^5D_0$–$^7F_2$, $^5D_0$–$^7F_3$, and $^5D_0$–$^7F_4$ transitions within Eu^{3+} ion, as is often the case with phosphors synthesized by the co-precipitation method [20]. However, when Dy dopants were added, the phosphors showed the luminescent peak at 590, 616, 650, and 700 nm, corresponding to the emission from Eu^{3+}, as well as peaks at 482 and 572 nm, attributed to the emission from Dy^{3+}, respectively. These results indicate that the luminescent properties of the phosphors could be tailored by addition of Dy.

Conclusion. We herein demonstrated that the red and yellow light-emitting Eu^{3+}/Dy^{3+} co-doped HA/TCP phosphor were synthesized successfully by the co-precipitation method followed by thermal annealing up 1100°C. In particular, the luminescence of the phosphors was significantly affected by annealing temperature and times. Moreover, under suitable excitation wavelength, the phosphors exhibited the characteristic emission of the dominant Eu^{3+} at about 590, 616, 650, and 700 nm with the additional emission center of Dy^{3+} at about 482 and 572 nm. These findings suggest that the combination of Eu^{3+} and Dy^{3+} in the host is very useful to achieve red and yellow single phosphors, which is of particular importance for potential applications in agriculture such as plant cultivation where a combination of red and yellow light is required for stimulating the fruit production.

Acknowledgment. This research is funded by Hanoi University of Science and Technology.

REFERENCES

1. Y. J. Zhang, Z. Y. Mao, D. J. Wang, J. Zhao, *Mater. Res. Bull.*, **67**, 1–4 (2015).
2. L. Ma, D. J. Wang, Z. Y. Mao, Q. F. Lu, Z. H. Yuan, *Appl. Phys. Lett.*, **93**, 144101–144101-3 (2008).
3. J. Chen, C. Guo, Z. Yang, T. Li, J. Zhao, *J. Am. Ceram. Soc.*, **99**, 218–225 (2016)
4. A. Shimada, Y. Taniguchi, *J. Photochem. Photobiol. B: Biol.*, **104**, 399–404 (2011).

5. I. Vänninen, D. M. Pinto, A. I. Nissinen, N. S. Johansen, L. Shipp, *Annu. Appl. Biol.*, **157**, 393–414 (2010).
6. Y. Wang, K. M. Folta, *Am. J. Bot.*, **100**, 70–78 (2013).
7. R. M. Klein, P. C. Edsall, *Photochem. Photobiol.*, **6**, 841–850 (1967).
8. U. V. Pedmale, S. C. Huang, M. Zander, B. J. Cole, J. Hetzel, K. Ljung, P. A. B. Reis, P. Sridevi, K. Nito, J. R. Nery, J. R. Ecker, J. Chory, *Cell*, **164**, 1–13 (2016).
9. A. Takemiya, S. I. Inoue, M. Doi, T. Kinoshita, K. I. Shimazaki, *The Plant Cell*, **17**, 1120–1127 (2005).
10. H. A. H. Graham, D. R. Decoteau, *Sci. Horticulturae*, **69**, 41–49 (1997).
11. K. E. Gerhardt, M. A. Lampi, B. M. Greenberg, *Photochem. Photobiol.*, **84**, 1445–1454 (2008).
12. G. Tamulaitis, P. Duchovskis, Z. Bliznikas, K. Breiv, R. Ulinskait, A. Brazaityt, A. Novičkovas, A. Zukauskas, *J. Phys. D: Appl. Phys.*, **38**, 3182–3187 (2005).
13. S. D. Gupta, B. Jatothu, *Plant Biotechnol. Rep.*, **7**, 211–220 (2013).
14. N. Yeh, J. P. Chung, *Renew. Sustain. Energ. Rev.*, **13**, 2175–2180 (2009).
15. L. Poulet, G. D. Massa, R. C. Morrow, C. M. Bourget, R. M. Wheeler, C. A. Mitchell, *Lif. Sci. Space Res.*, **2**, 43–53 (2014).
16. Y. Xie, W. He, F. Li, T. S. H. Perera, L. Gan, Y. Han, X. Wang, S. Li, H. Dai, *ACS Appl. Mater. Interfaces*, **27**, 10212–10219 (2016).
17. K. Hasna, S. S. Kumar, M. Komath, M. R.Varma, M. K. Jayaraj, K. R. Kumar, *Phys. Chem. Chem. Phys.*, **15**, 8106–8111 (2013).
18. A. K. S. Lafarga, F. P. P. Moisés, A. Gurinov, G. G. Ortiz, G. G. C. Arízaga, *Mater. Sci. Eng. C*, **48**, 541–547 (2015).
19. C. Rosticher, B. Viana, T. Maldiney, C. Richard, C. Chanéac, *J. Lumin.*, **170**, 460–466 (2016).
20. V.H. Pham, N. N. Trung, *Mater. Lett.*, **36**, 359–361 (2014).
21. C. X. Thang, V. H. Pham, *Mater. Sci. Eng. B*, **197**, 18–24 (2015).
22. T. C. Xuan, N. N. Trung, V. H. Pham, *Optik*, **126**, 5019–5021 (2015).
23. Y. Han, X. Wang, H. Dai, S. Li, *J. Lumin.*, **135**, 281–287 (2013).
24. F. R. O. Silva, N. B. de Lima, A. H. A. Bressiani, L. C. Courrol, L. Gomes, *Opt. Mater.*, **47**, 135–142 (2015).
25. S. Huang, J. Zhu, K. Zhou, *Mater. Res. Bull.*, **47**, 24–28 (2012).